

Original Research Article

# Synthesis and Characterization of Heterocyclic Derivatives to Evaluate their Efficiency as Corrosion Inhibitors for Carbon Steel in Saline Medium

Wadhah Naji Al-Sieadi<sup>ID</sup>, Oday H. R. Al-Jeilawi<sup>ID</sup>, Noor Ali Khudhair<sup>ID</sup>, Andy N. S. Shamaya<sup>ID</sup>, Nadia A. Abdulrahman\*<sup>ID</sup>

University of Baghdad, College of Sciences, Department of Chemistry, Baghdad, Iraq

## ARTICLE INFO

### Article history

Submitted: 19 June 2024

Revised: 30 July 2024

Accepted: 19 August 2024

ID: [AJCA-2407-1601](https://doi.org/10.48309/AJCA-2407-1601)DOI: [10.48309/AJCA.2025.468574.1601](https://doi.org/10.48309/AJCA.2025.468574.1601)

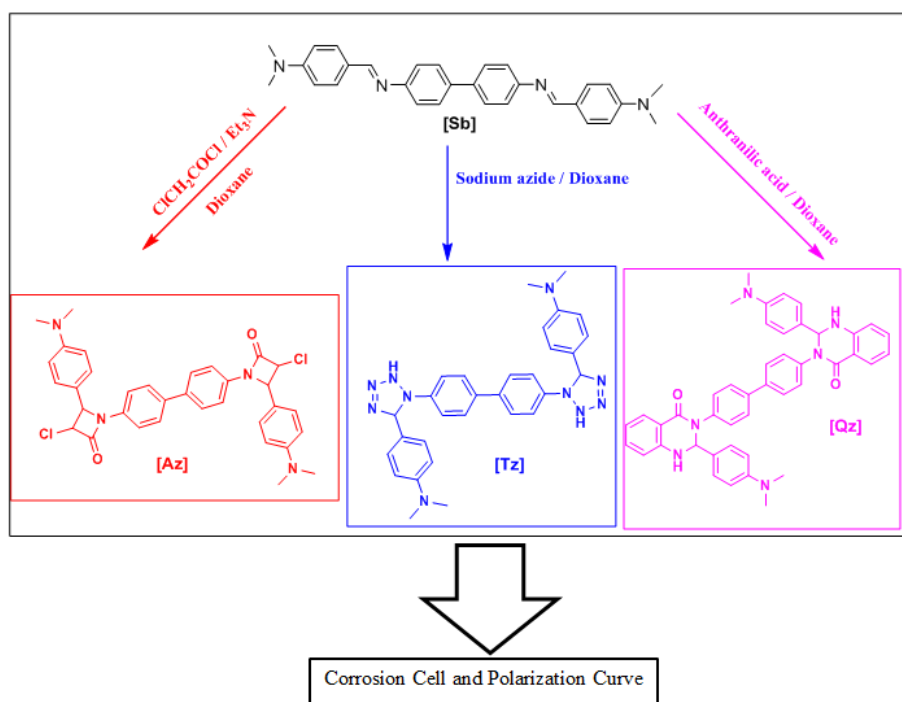
### KEYWORDS

Corrosion inhibition  
Heterocyclic rings  
Corrosion cell  
Polarization curve

## ABSTRACT

This work includes preparation of Az, Qz, and Tz derivatives from the reaction of Schiff base (Sb) derivative with anthranilic acid, chloroacetyl chloride, and sodium azide, as well as, the characterization via FT-IR, <sup>1</sup>H-NMR, and <sup>13</sup>C-NMR. The anticorrosion inhibition of these compounds was studied and the measurements of carbon steel (CS) corrosion in sodium chloride solution 3.5% (blank) and inhibitor in solutions were calculated at a temperature range of 293-323 K by the technique of electrochemical polarization. In addition, some thermodynamic and kinetic activation parameters for inhibitor and blank solutions ( $E_a^*$ ,  $\Delta H^*$ ,  $\Delta S^*$ , and  $\Delta G^*$ ) were determined. The results showed high inhibition efficacy for all the prepared compounds, the maximum of which was in compounds Sb and Az with an inhibition rate of 99% at all temperatures. However, the percentage decreased in other compounds, as it varied and decreased with the increasing of temperatures.

## GRAPHICAL ABSTRACT



\* Corresponding author: Abdulrahman, Nadia A.

✉ E-mail: [nadia.abdulrahman@sc.uobaghdad.edu.iq](mailto:nadia.abdulrahman@sc.uobaghdad.edu.iq)

© 2025 by SPC (Sami Publishing Company)

## Introduction

The deterioration of materials caused by their interaction with the environment is known as corrosion, and corrosion of most metals and other materials cannot be avoided. Corrosion is a ubiquitous phenomenon and there is no way to completely stop it. Some new solutions can only slow down the process. Corrosion has two electrochemical reactions, oxidation occurs on the anodic side, reduction occurs on the cathodic side, and in acidic media the hydrogen evolution reaction dominates, and corrosion inhibitors reduce or prevent these reactions [1]. Pollution, global warming, and climate change are direct causes of rising corrosion costs. Damages due to corrosion include the cost of repairing or replacing corroded parts or equipment [2-5].

Generally speaking, one of the most practical ways to protect metals from corrosion in acidic media is the use of corrosion inhibitors such as the chemical inhibitors. The use of chemical inhibitors to slow down the rate of the corrosion process is varied. The chemical inhibitors may also include the nano materials which could be easily prepared via un-expansive methods; with and without the effect of magnetic field. Corrosion inhibitors have been considered for long time as the first line of defense against corrosion in the petroleum production and refining industry [6-11]. The interaction of the metal's surface with heteroatoms [12-14] like sulfur, nitrogen, and oxygen [15] plays an important role in corrosion inhibition due to the presence of lone pairs of electrons [16]. The choice of inhibitors is based on two considerations, one is economic considerations, and the other is that relatively long-chain

compounds ought to contain an electron clouds on electronegative atoms like N and O or the aromatic ring [17].

Preparation of Az, Qz, and Tz derivatives from the reaction of Schiff base (Sb) derivative with anthranilic acid, chloroacetyl chloride, and sodium azide is performed in this work, and then anti-corrosion inhibition of these compounds was studied and the measurements of carbon steel (CS) corrosion in sodium chloride solution 3.5% (blank) and inhibitor in solutions were calculated by the technique of electrochemical polarization.

## Materials and Methods

### Materials

#### Corrosion measurement

A host, thermostat, magnetic stirrer, EmStat 4s, Palm Sens, Holland potentiostat, and galvanostat are made up the potentiostat assembly. The cell has a limit of 250 mL, is made of pyrex glass and comprises of an inward shell and an external shell. Three electrodes comprise an electrochemical corrosion cell. Platinum serves as the auxiliary electrode and carbon steel serves as the working electrode (Table 1), the length was 10 cm, the reference electrode was saturated calomel (Hg/Hg<sub>2</sub>Cl<sub>2</sub> sat. KCl), and was immersed for 15 minutes in the test solution to measure the steady-state open circuit potential of the working electrode. (Eocp), and then electrochemical measurements were carried out with a potential of less than ( $\pm 200$ ) mV. All experiments were carried out at different temperatures using hot and cold circulating water baths [18].

**Table 1.** Composition of carbon steel C45 chemical

Metal	C%	Si%	Mn%	S%	P%	Cu%	Ni%	Cr%	Fe%
Carbon Steel 45	0.36-0.42	0.15-0.30	1.00-1.40	0.05	0.05	0.50	0.20	0.20	96.88-97.49

## Description of corrosion system

### Corrosion cell

The Pyrex corrosion cell (250 mL) volume consists of two containers, an inner and an outer. A corrosion cell and three electrodes are shown. Three electrodes and a thermostat are replaced in the inner tube [19]. The three electrodes can be explained as follows:

A. *The electrode of reference* is used to check that the working electrode's potential matches that of the reference electrode. The reference electrode potential is well-known and accurate. It is composed of two tubes; Hg/Hg<sub>2</sub>Cl<sub>2</sub> sat. KCl is contained in the inner tube and the working electrode is 2 millimeters away from the reference electrode.

B. *The additional electrode* is made of high-impurity metal platinum, of which its length is 10 centimeters.

C. *The electrode that works* is the research object and its potential should be measured. The electrode is formed from a 20 cm long metal wire and connected to the mounted sample.

The tested samples were placed in a corrosion bath in which the surface that was exposed to the solution had a diameter of 16.55 cm<sup>2</sup>.

### Methods

#### *N, N'-Bis (4-(dimethylamino) benzylidene) biphenyl-4, 4'-diamine (Sb) [20]*

*P*-(Dimethylamino) benzaldehyde (1.2 mg, 0.008 mol) and 3 to 4 drops of gla. Acetic acid in 10 mL of abs.ethanol was stirred for (5 minutes), and then a solution of Benzidine (0.74 gm, 0.004 mole) in absolute ethanol (15 mL) was cautiously added. The mixture was refluxed and stirred for about 1 hour, the mixture was then poured into crushed ice, and the precipitate was filtered, and in the ethanol was re-crystallized.

Yellow precipitate; yield (80%); M.P = (327-330) °C; FT-IR (KBr)  $\nu$ , cm<sup>-1</sup>: 3015 (C-H)

aromatic, 2920,2850 (C-H) aliphatic, 1612 (C=N), 1469 (C=C) aromatic, and 1357 (C-N); <sup>1</sup>H-NMR (500 MHz, DMSO-*d*<sub>6</sub>)  $\delta$ <sub>H</sub>, ppm: 3.31 (12 H, s, CH<sub>3</sub>), 6.53-7.85 (16H, m, H aromatic), 8.47-8.92 (2H, s, CH=N); <sup>13</sup>C -NMR (125.5 MHz, DMSO-*d*<sub>6</sub>)  $\delta$ <sub>C</sub>, ppm: 45.7 (CH<sub>3</sub>), 124.6-150.21 (C aromatic), and 164.72 (C=N).

#### *1, 1'-([1, 1'-Biphenyl]-4, 4'-diyl) bis (3-chloro-4-(4-(dimethylamino) phenyl) azetid-2-one) (Az) [21]*

A solution of Schiff-base (Sb) (0.22 mg, 0.0005 mol) in dioxane (20 mL) was added to the mixed chloro acetyl chloride mixture. (0.08 mL, 0.001 mol) and Et<sub>3</sub>N (0.14 mL, 0.001 mol) in dioxane (5 mL) at 0-5°C. The mixture was refluxed for 25 hours and kept at room temperature for two days. After that, the mixture from the reaction was poured into crushed ice and filtered through a water wash. Ethanol was used to dry and recrystallize the solid product.

Light-Yellow precipitate; yield (65%); M.P. = 244-246 °C; FT-IR (KBr)  $\nu$ , cm<sup>-1</sup>: 3011 (C-H) aromatic, 2915, 2830 (C-H) aliphatic, 1674 (C=O), 1457 (C=C) aromatic, and 1370 (C-N); <sup>1</sup>H-NMR (500 MHz, DMSO-*d*<sub>6</sub>)  $\delta$ <sub>H</sub>, ppm: 3.29 (12 H, s, CH<sub>3</sub>), 5.25 (2H, d, CH-N), 5.53 (2H, d, CH-Cl), and 6.74-7.78 (16H, m, H aromatic); <sup>13</sup>C-NMR (125.5 MHz, DMSO-*d*<sub>6</sub>)  $\delta$ <sub>C</sub>, ppm: 42.5 (CH<sub>3</sub>), 63.8 (C-Cl), 69.3 (C-N), 112.4-149.7 (C aromatic), and 161.62 (C=O).

#### *3, 3'-[1, 1'-Biphenyl]-4, 4'-diyl] bis (2-(4-(dimethylamino) phenyl)-2, 3-dihydroquinazolin-4(1H)-one) (Qz) [22]*

A solution of Schiff-base (Sb) (0.22 mg, 0.0005 mol) in dioxane (20 mL); anthranilic acid (0.14 mg, 0.001 mol) was added. After that, the mixture refluxed for 23 hours at the end of the reaction, the mixture was powered into ice cold water and let to precipitate, filtrate, dried, and recrystallized from ethanol. Yellow precipitate; yield (70%); M.P. = 302-304 °C; FT-IR (KBr)  $\nu$ , cm<sup>-1</sup>: 3119 (N-H), 3021 (C-H) aromatic,

2919,2845 (C-H) aliphatic, 1671 (C=O), 1453 (C=C) aromatic, and 1382 (C-N);  $^1\text{H-NMR}$  (500 MHz, DMSO- $d_6$ )  $\delta_{\text{H}}$ , ppm: 3.17 (12 H, s, CH<sub>3</sub>), 5.98 (2H, d, CH-N), 6.31 (2H, d, N-H), and 6.5-7.89 (24H, m, H aromatic);  $^{13}\text{C-NMR}$  (125.5 MHz, DMSO- $d_6$ )  $\delta_{\text{C}}$ , ppm: 40.05 (CH<sub>3</sub>), 84.5 (C-N), 119.2-151.3 (C aromatic), and 160.5 (C=O).

4, 4'-([1, 1'-Biphenyl]-4, 4'-diylbis (2, 5-dihydro-1H-tetrazole-1, 5-diyl)) bis (N, N-dimethylaniline) (Tz) [23]

The solution of sodium azide (0.065 mg, 0.001 mol) was dissolved in dioxane (10 mL) and added to the solution of Schiff base (Sb) (0.22 mg, 0.0005 mol) in dioxane (20 mL). The mixture was refluxed for the required 25 hours. Before being recrystallized with ethanol, the product was thoroughly rinsed with cold water after the solvent was removed.

Light-Gray precipitate; yield (75%); M.P = 204-206 °C; FT-IR (KBr)  $\nu$ , cm<sup>-1</sup>: 3217 (N-H), 3002 (C-H) aromatic, 2917, 2865 (C-H) aliphatic, 1465 (C=C) aromatic, 1418 (N=N), and 1361 (C-N);  $^1\text{H-NMR}$  (500 MHz, DMSO- $d_6$ )  $\delta_{\text{H}}$ , ppm: 3.12 (12 H, s, CH<sub>3</sub>), 3.6 (1H, s, NH), 4.3 (1H, s, CH-N), and 6.62-7.94 (16H, m, H aromatic);  $^{13}\text{C-NMR}$  (125.5 MHz, DMSO- $d_6$ )  $\delta_{\text{C}}$ , ppm: 42.7 (CH<sub>3</sub>), 95.4 (C-N), and 111.3-149.63 (C aromatic).

## Results and Discussion

### Organic inhibitors

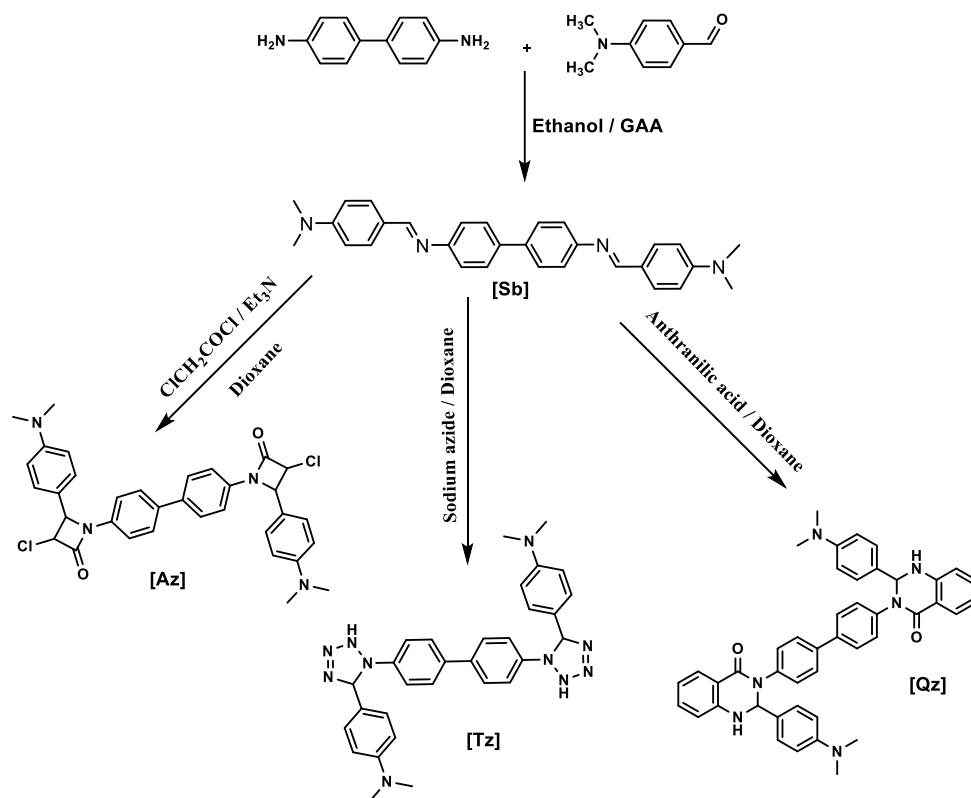
The derivatives in Scheme 1 were prepared by conducting a Schiff-Base reaction between Benzidine and *p*-(*N,N*-dimethyl amino) benzaldehyde using two moles from the last compound to prepare the derivative Sb, where it was observed that the amine and aldehyde groups disappeared and the appearance of imine group (CH=N) represented by the following spectroscopic measurements [24,25], FT-IR at 1612 cm<sup>-1</sup>;  $^1\text{H-NMR}$  at 8.47,8.92 (2H, s) ppm ;  $^{13}\text{C-NMR}$

164.72 ppm. Several ring-closure reactions were carried out on the derivative Sb, which led to the disappearance of the imine group, including its reaction with chloro acetyl chloride in Et<sub>3</sub>N presence to prepare the derivative Az, where the presence of a carbonyl for amide group (C=O) was observed, which showed the following results FT-IR at 1674 cm<sup>-1</sup>;  $^{13}\text{C-NMR}$  at 161.62 ppm. Likewise, the derivative Qz was prepared by the reaction of Sb with anthranilic acid, and the appearance of each of the following groups was detected FT-IR at 3119 and 1671 cm<sup>-1</sup> for (N-H) and (C=O), respectively;  $^1\text{H-NMR}$  6.31 ppm (2H, d, N-H);  $^{13}\text{C-NMR}$  160.5 ppm for (C=O). In another line, the imine group was closed in compound Sb with sodium azide, and the resulting compound Tz was detected by the appearance bands at 3217 and 1418 cm<sup>-1</sup> for (N-H) and (N=N) groups;  $^1\text{H-NMR}$  3.6 ppm for NH (1H, s) and 4.3 ppm (1H, s, CH-N).

### Polarization curves

The data in Table 2 and Figures 1-3 were utilized to assess the corrosion parameters. The corrosion potential ( $E_{\text{corr}}$ ) and current density ( $i_{\text{corr}}$ ) were determined by extrapolating the cathodic and anodic tafel in the presence and absence of inhibitor molecules in a NaCl 3.5% solution. Furthermore, the anodic (ba) and cathodic (bc) tafel slopes were computed. Information on the cathodic and anodic tafel slopes (mV/Dec) is among the findings, protection efficiency PE%, corrosion potential  $E_{\text{corr}}$  (mV), corrosion current density  $i_{\text{corr}}$  (A/cm<sup>2</sup>). According to the tafel plot,  $E_{\text{corr}}$  for C.S. shifts to a higher (noble) position when the inhibitors are present compared to the blank solution, indicating that the protection acts as an anodic protection. Equation 1 [26] was used to compute the inhibitory efficiency (%IE):

$$\%IE = \frac{(i_{\text{corr}})_o - (i_{\text{corr}})}{(i_{\text{corr}})_o} * 100 \quad (1)$$



**Scheme 1.** Preparation of organic inhibitors.

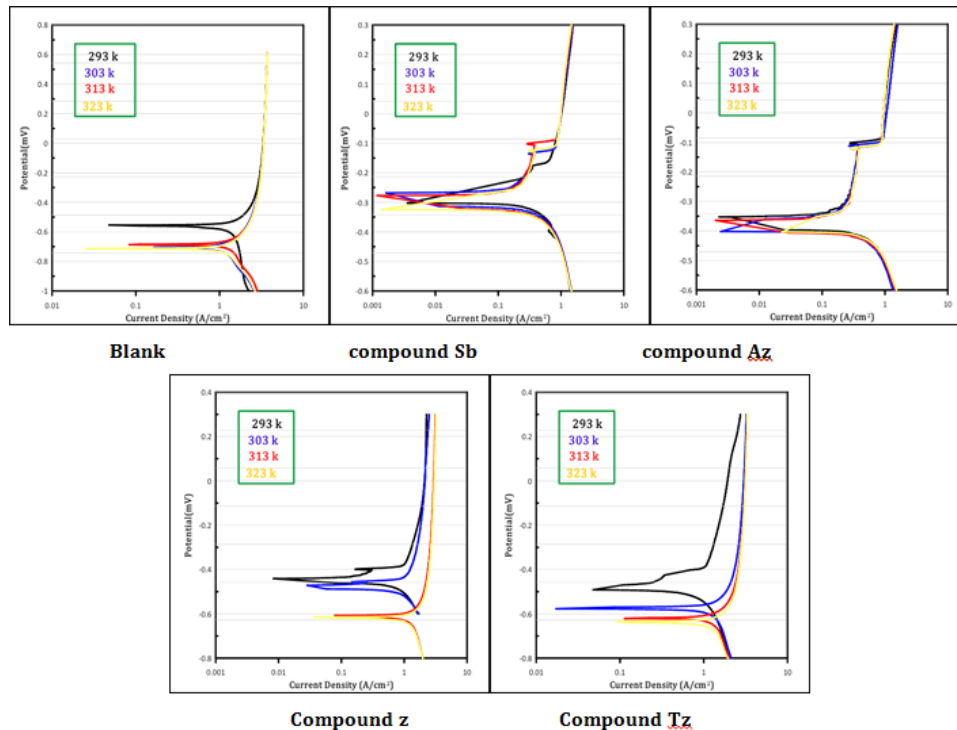


**Figure 1.** Polarization curves for the corrosion of organic inhibitors and a blank 3.5% NaCl solution at various temperatures.

**Table 2.** Parameters of corrosion for the compound and blank in NaCl solutions at various temperatures

Compound	Temp.	E <sub>corr.</sub>	I <sub>corr.</sub>	I <sub>corr.</sub> / r	Resis.	Anodic β	Cathodic β	Corr. rate,	IE%
Blank	293	-1.031	134.1	1.341E-4	1293	0.874	0.735	0.658	
	303	-0.917	144.5	1.445E-4	463.9	0.791	0.192	0.709	
	313	-0.880	153.9	1.539E-4	395.4	0.739	0.173	0.755	
	323	-0.914	160.2	1.602E-4	406.4	0.799	0.185	0.786	
Sb	293	-0.295	1.355	1.355E-6	4.893E+4	0.827	0.187	0.007	99
	303	-0.279	1.508	1.508E-6	3.770E+4	0.322	0.221	0.007	99
	313	-0.306	1.738	1.738E-6	4.547E+4		0.198	0.009	99
	323	-0.215	1.855	1.855E-6	5.049E+4	0.668	0.319	0.009	99
Az	293	-0.383	1.580	1.580E-6	3.366E+4	1.404	0.134	0.008	99
	303	-0.336	1.667	1.667E-6	5.184E+4	1.257	0.236	0.008	99
	313	-0.363	1.760	1.760E-6	4.190E+4	1.619	0.190	0.009	99
	323	-0.347	1.801	1.801E-6	4.350E+4	1.641	0.203	0.009	99
Qz	293	-0.460	5.602	5.602E-6	7909	0.288	0.158	0.027	96
	303	-0.496	6.786	6.786E-6	5162	0.249	0.119	0.033	95
	313	-0.616	10.74	1.074E-5	2070	0.089	0.121	0.053	93
	323	-0.621	15.84	1.584E-5	1930	0.104	0.216	0.078	90
Tz	293	-0.477	7.577	7.577E-6	9827	0.438	0.282	0.037	94
	303	-0.571	15.92	1.592E-5	2140	0.119	0.232	0.078	89
	313	-0.619	19.24	1.924E-5	1790	0.115	0.254	0.094	87
	323	-0.660	22.72	2.272E-5	1805	0.150	0.254	0.111	86

Where, ( $i_{corr}$ )<sub>o</sub> is the corrosion current density without inhibitors ( $i_{corr}$ ) is different from the corrosion current density with inhibitors [27]. E corrosion: V, I corrosion:  $\mu$ A, I corrosion per surface area: A/cm<sup>2</sup>, Polarization Resistance:  $\Omega$ , Anodic  $\beta$  Tafel constant: V/decade, Cathodic  $\beta$  Tafel constant: V/decade, Corrosion rate: mm/year, and IE%: inhibition efficiency.

#### Kinetic and thermodynamic activation parameters

According to calculations made using the Clausius-Clapeyron and Arrhenius Equation 2 and its alternate formulation, known as the transition state, the activation energy  $E_a^*$ , the activation enthalpy  $\Delta H^*$ , and the activation entropy  $\Delta S^*$  were the thermodynamic activation parameters [28].

$$\log \frac{I_{corr.2}}{I_{corr.1}} = \frac{\Delta H^*}{2.303R} + \frac{(T_2 - T_1)}{T_2 T_1} \quad (2)$$

Where,  $I_{corr}$  describes corrosion rate, ( $\Delta H^*$ : enthalpy of activation =  $E_a^*$ : Activation energy), R: Gas constant (8.315 JK<sup>-1</sup>mol<sup>-1</sup>), and T: Absolute temperature (K). While, the transition state is expressed in Equation 3 [23]:

$$\log \frac{I_{corr.}}{T} = \log \left[ \frac{R}{N h} + \frac{\Delta S^*}{2.303R} \right] - \frac{\Delta H^*}{2.303RT} \quad (3)$$

Where, N: Avagadrous number ( $6.022 \times 10^{23}$ mol), h: Planks constant ( $6.62 \times 10^{-34}$  J.S), and  $\Delta S^*$ : the entropy of activation and enthalpy of activation. The free energy of activation was determined from Equation 4 [29]:

$$\Delta G^* = \Delta H^* - T\Delta S^* \quad (4)$$

According to the findings, the thermodynamic activation parameters ( $E_a^*$  and  $\Delta H^*$ ) were often



higher than those of an unprotected system [30]. At greater temperatures, the inhibitor molecule coverage of the metal surface may increase, which could account for this. This suggests that the rate at which the chemisorbed layer forms may be faster than its rate of dissolution at high temperatures. According to different viewpoints, some inhibitors in aqueous solutions alter the corrosion reaction's kinetics by suggesting alternative reaction pathways with lower activation energies. This tendency helps to slow down the rate of metal corrosion [18].

The fact that  $\Delta S^*$  is negative in both the presence and absence of the inhibitor demonstrates that the activation process is more concerned with the association stage than it is

with the dissociation stage [31]. In other words, as indicated in Table 3, during the transition from reactant to active complex, the free energy activation decreases. With a rise in temperature, there is essentially no change visible, indicating that the activated complex was unstable and that there was less chance of its production as the temperature rose [32].

When the inhibitors are present, the C.S.'s ( $E_{corr}$ ) changes to a higher position compared to the blank solution, which suggests that the inhibitors serve as an anodic safeguard and inhibition efficiency (IE%) indicate that the inhibitor form with metal a complex that adsorb on the surface of alloy and protect it from corrosive media [33].

**Table 3.** Thermodynamic parameters of the transition state at various temperatures for the corrosion of blank and inhibitor solutions at temperatures between 293 and 323 K

Sample	T(K)	Ea (kJ/mole)	$\Delta H^\ddagger$ (kJ/mol)	$\Delta S^\ddagger$ (kJ/mol.K)	$\Delta G^\ddagger$ (kJ/mol)
Blank	293	4.709	2.152	-0.196	59.58
	303				61.54
	313				63.5
	323				65.46
Sb	293	8.547	5.991	-0.173	56.68
	303				58.41
	313				60.14
	323				61.87
Az	293	3.531	0.974	-0.157	46.975
	303				48.545
	313				50.115
	323				51.685
Qz	293	28.032	25.476	-0.144	67.668
	303				69.108
	313				70.548
	323				71.988
Tz	293	27.696	25.139	-0.140	66.159
	303				67.559
	313				68.959
	323				70.359

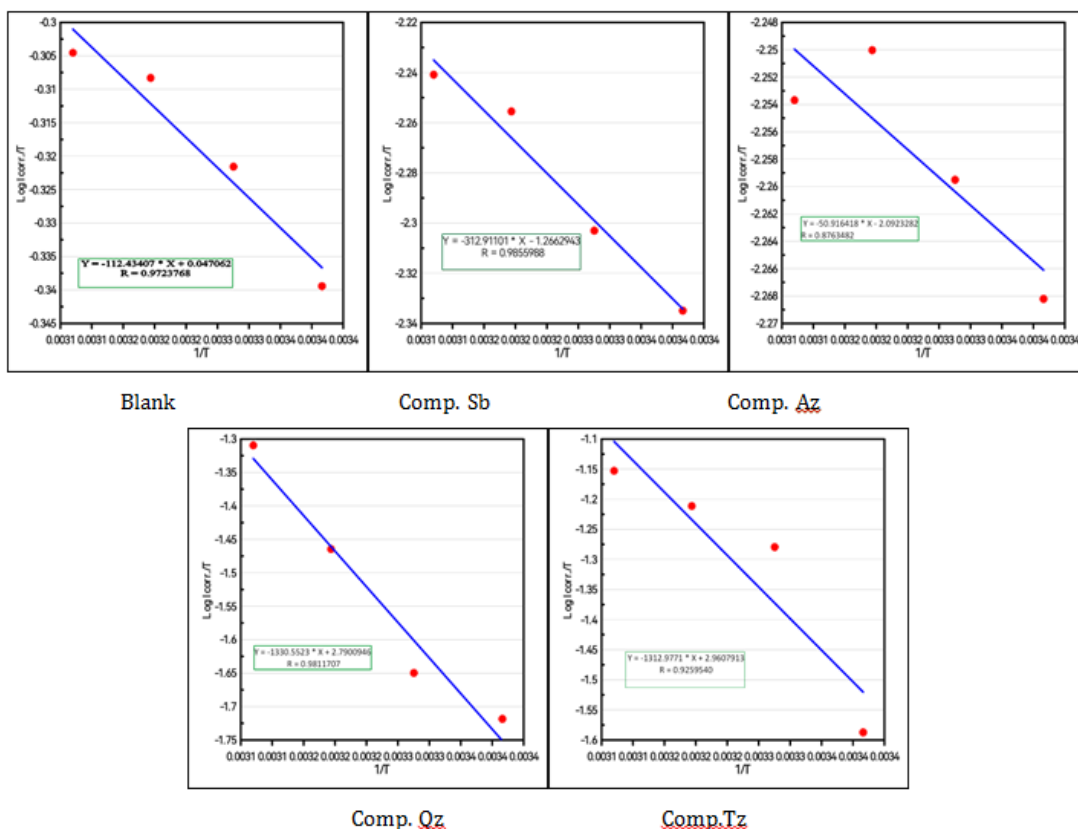


Figure 2. Plot of  $\log I_{\text{corr.}}/T$  vs.  $1/T$  for organic inhibitors

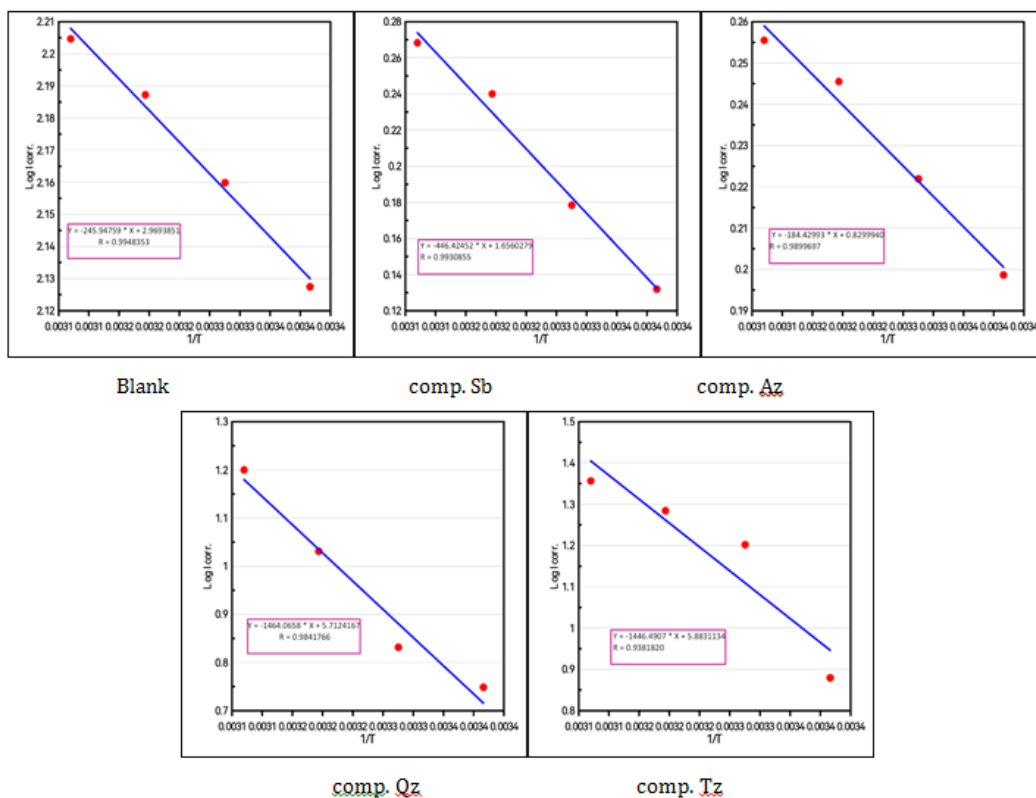


Figure 3. Plot of  $\log icorr.$  vs.  $1/T$  for organic inhibitors



## Conclusion

To sum up, the reaction of Schiff base (Sb) derivative with anthranilic acid, chloroacetyl chloride, and sodium azide performed to produce Az, Qz, and Tz derivatives. Polarization curves for the corrosion of organic inhibitors, kinetic and thermodynamic activation parameters, and the related plots are investigated. The results showed high inhibition efficacy for all the prepared compounds, the maximum of which was in compounds Sb and Az with an inhibition rate of 99% at all temperatures. However, the percentage decreased in other compounds; as it varied and decreased with the increasing of temperatures.

## Conflict of interest

The authors declare that they have no conflicts of interest in this study.

## Orcid

Wadhah Naji Al-Sieadi : 0009-0006-6810-7623

Oday H. R. Al-Jeilawi : 0000-0002-4092-2072

Noor Ali Khudhair : 0000-0003-0238-4952

Andy N. S. Shamaya : 0009-0002-1580-096X

Nadia A. Abdulrahman : 0000-0001-8142-2990

## References

- [1] M.T. Mohammed, W.N. Al-Sieadi, O.H. Al-Jeilawi, Characterization and synthesis of some new schiff bases and their potential applications, *Eurasian Chemical Communications*, **2022**, *4*, 481-494. [[Crossref](#)], [[Google Scholar](#)], [[Publisher](#)]
- [2] A. Al-Zahra, H.N. Al-Ani, O.H. AL-Jeilawi, Experimental and theoretical study of 3-benzyl -2-mercaptoquinoizoline-4(3H)-one (BMQ) as an inhibitor of carbon steel corrosion in acidic media, *International Journal of Science and Nature*, **2018**, *9*, 105-113. [[Google Scholar](#)]
- [3] N.A. Khudhair, I.M.H. Al-Mousawi, N.A. Abdulrahman, Extracting ellagic acid from the pomegranate fruit peels and its application as an inhibitor of carbon steel 45 corrosion in different media, *Advanced Journal of Chemistry, Section A*, **2024**, 820-833. [[Crossref](#)], [[Publisher](#)]
- [4] S. Bais, Fabrication of electrochemically deposited zinc rich Ni-Co-Zn alloy coatings reinforced with pyridine and investigation of their anticorrosion performance in acidic medium, *Advanced Journal of Chemistry, Section A*, **2024**, *7*, 550-564. [[Crossref](#)], [[Publisher](#)]
- [5] Z.K. Kuraimid, A.E.A.S. Fouda, D.S. Abid, Static and dynamic study of novel 4-formyl-N-hexadecyl-N, N-dimethylbenzenaminium bromide synthesized as a corrosion inhibitor use in petroleum wells acidizing process, *Chemical Methodologies*, **2023**, *7*, 552-568. [[Crossref](#)], [[Publisher](#)]
- [6] A.M. AL-Sammorraie, Role of carbon dioxide on the corrosion of carbon steel reinforcing bar in simulating concrete electrolyte, *Baghdad Science Journal*, **2020**, *17*, 0093-0093. [[Crossref](#)], [[Google Scholar](#)], [[Publisher](#)]
- [7] E. Heitz, W. Schwenk, Theoretical basis for the determination of corrosion rates from polarisation resistance: Report prepared for the european federation of corrosion working party on physicochemical testing methods of corrosion—fundamentals and application, *British Corrosion Journal*, **1976**, *11*, 74-77. [[Crossref](#)], [[Google Scholar](#)], [[Publisher](#)]
- [8] H.G. Hameed, N.A. Abdulrahman, Preparation and characterization of TiO<sub>2</sub> nanoparticles with and without magnetic field effect via hydrothermal technique, *Iraqi Journal of Science*, **2023**, *64*, 3225-3231. [[Crossref](#)], [[Google Scholar](#)], [[Publisher](#)]
- [9] S.T. Abdulredha, N.A. Abdulrahman, Cu-ZnO Nanostructures synthesis and characterization, *Iraqi Journal of Science*,

- 2021**, *62*, 708-717. [[Crossref](#)], [[Google Scholar](#)], [[Publisher](#)]
- [10] L. Mardare, L. Benea, Effects of TiO<sub>2</sub> nanoparticles on the corrosion protection ability of polymeric primer coating system, *Polymers*, **2021**, *13*, 614. [[Crossref](#)], [[Google Scholar](#)], [[Publisher](#)]
- [11] G. Zhang, J. Liu, Y. Zhu, T. Shen, D.-q. Yang, Enhanced antibacterial efficacies, corrosion resistance, and cytocompatibility of ZnO/CuO composite coatings through designed sputtering orders, *Applied Surface Science*, **2023**, *635*, 157724. [[Crossref](#)], [[Google Scholar](#)], [[Publisher](#)]
- [12] S. Thomas, N. Birbilis, M. Venkatraman, I. Cole, Corrosion of zinc as a function of pH, *Corrosion, The Journal of Science and Engineering*, **2012**, *68*, 015009-015001-015009-015009. [[Crossref](#)], [[Google Scholar](#)], [[Publisher](#)]
- [13] F. Hamouche, M.E. Touhami, Y. Hassani, Y. Baymou, Effect of cyclic temperature on the corrosion behavior of ( $\alpha + \beta$ )-Brass (CuZn<sub>36</sub>Pb<sub>2</sub>As) and  $\alpha$  brass (CuZn<sub>21</sub>Si<sub>3</sub>P) in tap water, *Journal of Applied Organometallic Chemistry*, **2024**, *4*, 30-50. [[Crossref](#)], [[Google Scholar](#)], [[Publisher](#)]
- [14] A.H. Hattab, S. Beebany, A.S. Kaki, The effect of H<sub>2</sub>SO<sub>4</sub> concentration on corrosion of Kirkuk's oil and gas pipelines with studying corrosion reaction rates kinetically, *Chemical Methodologies*, **2023**, *7*, 257-267. [[Crossref](#)], [[Google Scholar](#)], [[Publisher](#)]
- [15] F.S. de Souza, A. Spinelli, Caffeic acid as a green corrosion inhibitor for mild steel, *Corrosion Science*, **2009**, *51*, 642-649. [[Crossref](#)], [[Google Scholar](#)], [[Publisher](#)]
- [16] T. Hoar, Electrochemical principles of the corrosion and protection of metals, *Journal of Applied Chemistry*, **1961**, *11*, 121-130. [[Crossref](#)], [[Google Scholar](#)], [[Publisher](#)]
- [17] O.H. Al-Jeilawi, H.N. Al-Ani, A. Al-Zahra, K.T. Al-Sultani, Exploring the potential of quantum chemical calculations for synthesized quinazoline derivatives as superior corrosion inhibitors in acidic environment, *Physical Chemistry Research*, **2024**, *12*, 205-217. [[Crossref](#)], [[Google Scholar](#)], [[Publisher](#)]
- [18] O.H. Al-Jeilawi, M.A. Al-Yassiri, Synthesis, Characterization and quantum mechanical study of some new 2-benzylidenehydrazinecarbothioamide derivatives as corrosion inhibitors for carbon/mild steel in acidic medium, *Iraqi Journal of Science*, **2015**, *56*, 1-11. [[Crossref](#)], [[Google Scholar](#)], [[Publisher](#)]
- [19] A.N.S. shamaya, O.H.R. Al-Jeilawi, N.A. Khudhair, Novel synthesis of some *N*-hydroxy phthalimide derivatives with investigation of its corrosion inhibition for carbon steel in HCl solution, *Chemical Methodologies*, **2021**, *5*, 331-340, 2021. [[Crossref](#)], [[Publisher](#)]
- [20] W. Damdoom, O. Al-Jeilawi, Synthesis, characterization of formazan derivatives from isoniazid and study their antioxidant activity and molecular docking, *Russian Journal of Bioorganic Chemistry*, **2024**, *50*, 86-94. [[Crossref](#)], [[Google Scholar](#)], [[Publisher](#)]
- [21] A. N. S. Shamaya and O. H. R. Al-Jeilawi, Organic synthesis of some new compounds derived from furfural and their evaluation as antioxidants, *Journal of Medicinal and Chemical Sciences*, **2023**, *6*, 1065-1076. [[Crossref](#)], [[Google Scholar](#)], [[Publisher](#)]
- [22] O.H. Al-Jeilawi, S.H. Tuama, I.A. Hussein, A.N. Shamaya, Synthesis, characterization, and biological evaluation of new cyclic quinazoline derivatives as potential antibacterial and antifungal agents, *Doklady Chemistry, Springer*, **2024**, 27-34. [[Google Scholar](#)]
- [23] Z. Tashrifi, M.M. Khanaposhtani, B. Larijani, M. Mahdavi, Sodium azide: An inorganic nitrogen source for the synthesis of organic *N*-compounds, *ChemistrySelect*, **2021**, *6*, 13419-13433. [[Crossref](#)], [[Google Scholar](#)], [[Publisher](#)]
- [24] R.M. Silverstein, G.C. Bassler, Spectrometric identification of organic compounds, *Journal*

- of *Chemical Education*, **1962**, 39, 546. [Crossref], [Google Scholar], [Publisher]
- [25] R.L. Shriner, C.K. Hermann, T.C. Morrill, D.Y. Curtin, R.C. Fuson, The systematic identification of organic compounds, *John Wiley & Sons*, **2003**. [Google Scholar], [Publisher]
- [26] P. Pickup, R. Osteryoung, Electrochemical polymerization of pyrrole and electrochemistry of polypyrrole films in ambient temperature molten salts, *Journal of the American Chemical Society*, **1984**, 106, 2294-2299. [Crossref], [Google Scholar], [Publisher]
- [27] U.H. Al-Jeilawi, S.M. Al-Majidi, K.A. Al-Saadie, Corrosion inhibition effects of some new synthesized *N*-aroyl-*N*-Aryl thiourea derivatives for carbon steel in sulfuric acid media, *Al-Nahrain Journal of Science*, **2013**, 16, 80-93. [Google Scholar], [Publisher]
- [28] A.M. Fox, Quantum optics: An introduction, *Oxford University Press*, **2006**. [Google Scholar]
- [29] G.K. Anderson, Enthalpy of dissociation and hydration number of carbon dioxide hydrate from the Clapeyron equation, *The Journal of Chemical Thermodynamics*, **2003**, 35, 1171-1183. [Crossref], [Google Scholar], [Publisher]
- [30] O.H. Al-Jeilawi, Corrosion inhibition for carbon steel of benzimidazole derivatives synthesized in sulfuric acid solution, *International Journal of Science and Research (IJSR)*, **2017**, 6, 2032. [Google Scholar], [Publisher]
- [31] S. Al-Majidi, U. Al-Jeilawi, K. Al-Saadie, Synthesis and characterization of some 2-sulphanyl benzimidazole derivatives and study of effect as corrosion inhibitors for carbon steel in sulfuric acid solution, *Iraqi Journal of Science*, **2013**, 54, 789-802. [Google Scholar], [Publisher]
- [32] N. Perez, Electrochemistry and corrosion science, *Springer*, **2004**. [Crossref], [Google Scholar], [Publisher]
- [33] D. Koutsoyiannis, Clausius–Clapeyron equation and saturation vapour pressure: Simple theory reconciled with practice, *European Journal of Physics*, **2012**, 33, 295. [Crossref], [Google Scholar], [Publisher]

#### HOW TO CITE THIS ARTICLE

W.N. Al-Sieadi, O.H.R. Al-Jeilawi, N.A. Khudhair, A.N.S. Shamaya, N.A. Abdulrahman. Synthesis and Characterization of Heterocyclic Derivatives to Evaluate their Efficiency as Corrosion Inhibitors for Carbon Steel in Saline Medium. *Adv. J. Chem. A*, 2025, 8(2), 209-219.

DOI: [10.48309/AJCA.2025.468574.1601](https://doi.org/10.48309/AJCA.2025.468574.1601)

URL: [https://www.ajchem-a.com/article\\_203811.html](https://www.ajchem-a.com/article_203811.html)